CONF-75-195-E
E-0365
C75/08/21

#365

DIMUON PRODUCTION BY PIONS AND PROTONS*

Presented by Roy Weinstein

for

G. J. Blanar, C. F. Boyer, W. L. Faissler, D. A. Garelick†, M. W. Gettner, M. J. Glaubman, J. R. Johnson, H. Johnstad, M. L. Mallary, E. L. Pothier, D. M. Potter, M. T. Ronan, M. F. Tautz, E. von Goeler and Roy Weinstein

Northeastern University at Boston

Boston, MA 02115

ABSTRACT

Dimuon production is reported for the reaction $\pi^- + Fe \rightarrow \mu^+ + \mu^- +$ anything at 200 GeV and $p + Fe \rightarrow \mu^+ + \mu^-$ anything at 240 GeV. The $X_L \equiv P_L/P_{Beam}$ and $P_\perp$ dependences of ψ production are parameterized and fitted. For $X_L \geqq 0.5$, the ratio of the ψ production cross section for pions in iron to that for protons is found to be 7.4 ± 2. For the intermediate mass region, $1.2 \leqq M \leqq 2.5$ GeV, preliminary results are given for X_L, $P_\perp$ and $M_{\mu\mu}$ dependences.

INTRODUCTION

This report will be concerned with two reactions

$$\pi^- + Fe \rightarrow \mu^+ + \mu^- + \text{anything} \qquad (1)$$

and

$$p^+ + Fe \rightarrow \mu^+ + \mu^- + \text{anything} \qquad (2)$$

These reactions were studied as part of an experiment designed primarily to search for charmed mesons. Both reactions were studied at FNAL in the M2 beam line, using monoenergetic beams. Pions of 200 GeV and protons of 240 GeV were used. I will report today only on the dimuon study. The results of the charm search will be reported elsewhere.

Time was in unusually short supply in this experiment. It was accepted on December 31, 1974, and scheduled to run three weeks later. Much of the apparatus of the muon arm, shown in Fig. 1, had to be built. One particular problem was that no existing magnet could be obtained for the experiment. The gapless magnet shown was designed in three days and built in seven days. Due to its size, and the period occupied by construction, it was named "Genesis". After construction, the experiment was assembled, debugged and run in two additional calendar weeks. The data presented here represent 25 hours of data taking time with the π^- beam, and 20 hours with the proton beam.

Fig. 1

The M2 beam is monitored by several hodoscopes, Cerenkov and scintillation counters not shown in Fig. 1. These counters result in a beam known to $\delta P_B/P_B \sim 0.002$ in momentum, $\delta\theta \sim 0.2$ m rad in incident angle, and $\delta X \sim 1/16''$ and $\delta Y \sim 1/8''$ in position. The beam is steered into a 2.5 meter hadron absorber, composed of iron, which acts as a beam dump. The hadron absorber and the Genesis magnet absorb essentially all hadrons in their combined 5.6 meter path length. The magnet was run at 18.6 kilo Gauss, and had an active area of approximately 2' x 2'.

Tracking of the particles was accomplished with three wire spark chambers following the magnet, and an x,y proportional wire chamber between the magnet and the hadron absorber, as shown in Figure 1.

The trigger required a coincidence of two particles, one on each side of the beam (one in the M2 and M3 counters and the other in the M4 and M5 counters). It will be noted in Fig. 1 that this trigger has a vertical split. There is a split between the trigger counters which causes the acceptance of the apparatus to approach zero as the dimuon invariant mass approaches its minimum value. The trigger rate due to single particles was reduced by requiring a pulse height of 1.5 x minimum ionizing in both the M0 and M1 counters.

A large number of checks were performed on the data in order to be sure the behavior of the apparatus was as expected, and to establish confidence. Some examples will be given here.

1) In the XZ (non-bending) plane the tracks should extrapolate back to the origin. However, the multiple coulomb scattering in the iron results in a Gaussian distribution of reconstructed origins, X_r, around zero. We have calculated the expected σ for this scattering using a monte carlo calculation. Plotted as in Fig. 2 a Gaussian distribution will appear as a straight line. The results are in good agreement with a straight line. Also, the slope of the line indicates that the calculated σ is correct to 8%. The point in X_r^2/σ^2 at which we cut the data is also shown in Fig. 2. In order to provide a distance scale to the figure, we note that σ is $\sim$ 1 cm for P_μ = 100 GeV.

2) A similar reconstruction has been done in the Z coordinate. The average Z is in good agreement with that expected from absorption in iron. The variation in Z is in good agreement with the monte carlo scattering calculation. At the ψ mass, $\sigma_Z \sim 44$ cm.

Fig. 2.

3) Beam counters show single minimum ionizing pulses for the incident particle, with no observable double minimum ionizing enhancement.

4) M0 and M1 trigger counters show double minimum ionizing pulses, with no single minimum ionizing enhancement.

5) The magnet was calibrated and checked using monoenergetic muon beams of various momenta, which were obtained by closing the M2 beam line collimators between the first and second stage of the M2 beam optics. The mean momentum observed, after calibration, was in good agreement with the beam momentum, and the momentum resolution was in good agreement with the monte carlo calculation.

6) The mass resolution predicted by the monte carlo program and that observed for the ψ are in good agreement.

7) For a sample of data runs, the number of dimuon events per unit beam flux corrected for detection efficiency is constant and checks the stability of the apparatus.

8) The neutral background in the wire chambers is negligible.

9) Acceptance was calculated by both analytical and monte carlo methods. The results were in excellent agreement.

These and other checks have given us a high degree of confidence in both our understanding of the equipment, and in the accuracy of the analysis programs.

We will first discuss the experimental results for the ψ, and then for the lower mass region. The ψ results, in the main, have been previously published(2). The low mass results are preliminary.

ψ Results

Figures 3 and 4 show the dimuon invariant mass spectra produced by the π and p beams. The graphs exhibit data prior to acceptance correction. The higher mass regions are also shown multipled by 20. The solid curves show the results of a monte carlo calculation based upon a delta function resonance at the ψ mass. The enhancements in the data at 3.1 GeV are seen to be consistent with the monte carlo calculation. We interpret these enhancements as the ψ meson.(1)

Fig. 3 Fig. 4

In order to study the behavior of the ψ cross section we cut our data on the mass region $2.5 \leq M_{\mu\mu} \leq 3.7$ GeV. If we extrapolate the analytical fit (to be discussed later) of the lower mass region into the ψ region we

estimate that ~ 5% or less of the events labeled as ψ's are due to lower mass dimuons. Also, using known π and γ inclusive spectra, the ψ production by π's measured in this experiment, and measured photoproduction of ψ's[3], we estimate that ψ production by cascade processes is $\leq$ 6% of the observed ψ's. Observation of doubly charged dimuons sets a < 2% upper limit on the number of neutral dimuons from π and K decay. Finally, we estimate an upper limit of $\leq$ 10% due to noise associated with beam muons in the π data.

We have fitted the ψ data for $P_L \geq 90$ GeV/c to a parameterization of the cross section of the form

$$\frac{d^2\sigma}{dx_L dp_\perp^2} \alpha\ e^{-aX_L}\ e^{-bp_\perp^2} \qquad (3)$$

where p_L is the laboratory momentum of the dimuon, and $X_L \equiv p_L/p_{Beam}$. Table 1 gives results for a and b, for both π^- and proton beams. Fits to $\exp(-b'p_\perp)$ are also given. The cut at $p_L \geq 90$ GeV/c, where the acceptance is $\geq$ 15%, is made to avoid acceptances near zero. In the data above 90 GeV/c there are 104 pion produced ψ's, and 45 proton produced ψ's.

Figure 5 shows the spectra in dimuon p_L, from which the Table 1 values for a_π and a_p were obtained. The proton result of $a_p = 9.7 \pm 1.6$ may be compared to the result $\alpha = 10$ obtained by Knapp et al[4] for neutrons (no error given). The values are in good agreement. There are no earlier values of a_π to which we may compare.

We have fitted the form of Eq.(3) for both $p_\perp^2$ and $p_\perp$ in the exponent. Figure 6 shows the $p_\perp$ fit, (labeled b' in Table 1). Comparison to the published results of Ref (4) for neutrons, b = 2, is somewhat uncertain because of the lack of quoted errors in reference (2). The results could disagree by several standard deviations. However, at this conference, O'Halloran has reported an updated neutron value of b = 1.5, based on a larger data sample. Our result of 1.1 ± 0.3 is in good agreement with the new result independent of what the error may be in the neutron measurement. There are no available results to which we may compare the π data.

Fig. 5

Table 1

ψ Results ($2.5 \leq M_{\mu\mu} \leq 3.7$ GeV)

Cross section form	π^-	p^+
e^{-aX_L}	$a_\pi = 6.2 \pm 0.8$	$a_p = 9.7 \pm 1.6$
$e^{-bp_\perp^2}$	$b_\pi = (0.81 \pm 0.14)\ \mathrm{GeV}^{-2}$	$b_p = (1.1 \pm 0.3)\mathrm{GeV}^{-2}$
$e^{-b'p_\perp}$	$b'_\pi = (1.6 \pm 0.2)\mathrm{GeV}^{-1}$	$b'_p = (2.2 \pm 0.5)\mathrm{GeV}^{-1}$
* $(1 - X_L)^n$	$n_\pi \sim 1.9$	$n_p \sim 4.0$

*Preliminary fit.

We have more recently tried fitting our data to a form $d\sigma/dx_L \propto (1 - X_L)^n$. Approximate fitted values for this form are also given in Table 1. These fits were not completed at the time of this conference, hence no errors are assigned. Our data indicates $(d\sigma/dx_L)_p/(d\sigma/dX_L)_\pi = (1 - X_L)^{.2.1}$

One of the striking results of this experiment is obtained by comparing the normalized yields, for π and proton produced ψ's. Since 200 GeV π's and 240 GeV protons were used, we compare yields in comparable X_L ranges. For $X_L \geq 0.5$ we compare the probability of producing a ψ per incident proton, $P_p(\psi)$, to the probability per incident pion, $P_\pi(\psi)$. We find

$$R \equiv \frac{P_\pi(\psi)}{P_p(\psi)} = 7.2 \pm 1.9; \qquad (X_L \geq 0.5) \qquad (4)$$

The errors shown are statistical only. Systematic errors are estimated to be smaller, and are neglected.

Our experiment directly measures the probability of an incident beam particle producing a ψ meson (or a dimuon of other mass). For the pion beam we find the probability of producing dimuons from a ψ meson at $p_L \geq 90$ GeV ($X_L \geq 0.45$) is

$$P_\pi(\psi) = (1.58 \pm 0.79) \times 10^{-7}; \qquad (X_L \geq 0.45) \qquad (5)$$

In this result the random errors are only about 11%. However the systematic errors in normalization enter directly, and we estimate these to be about 50%.

Fig. 6 Fig. 7

For the proton beam we find the probability of producing dimuons from a ψ meson at $P_L \geq 90$ GeV ($X_L \geq 0.375$) is

$$P_p(\psi) = (0.59 \pm 0.30) \times 10^{-7}; \qquad (X_L \geq 0.375) \quad (6)$$

We may compare our proton results, Eq (6), to that of Knapp et al[4]. See Fig. 7. The results of Ref. 4 extrapolated to $X_L = .375$, are $P_n(\psi) = (0.17 {}^{+0.17}_{-0.09})$. (This uses the factor of 2 error quoted in Ref. 4. The errors quoted in the results of our experiment, Eq. 5 and 6, are lower in large part because of the relative ease of monitoring a beam of charged, monoenergetic particles compared to a markedly non-monoenergetic beam of neutrals.) Our production probabilities are about 3.6 times higher than that of Ref. 4.[5] However no discrepancy exists because of the large systematic errors present in the neutron measurement. If the factor of two error quoted in Ref 2 is used, the experiments disagree by $\Delta P(\psi) = (0.43 \pm 0.35) \times 10^{-7}$. O'Halloran has presented at this conference results with a slightly larger error estimate than Ref 4, and using this newer estimate we conclude that there is no evidence of a proton-neutron difference. Thus in the values of a_p, b_p, and absolute production probability, the neutron and proton data are presently consistent.

We may interpret Eqs. (5) and (6) in various ways by (a) assuming an A dependence of the ψ production cross section in nuclei, (b) assuming that the parameterization of Eq. 3 holds down to minimum X, and (c) using the branching ratio results of other experiments.

First, we find, using Eqs. 5 and 6 and a total inelastic iron cross section of $\sigma_{Fe} \approx 0.7$ barns that the cross section for producing ψ's in iron is

$$\sigma_{\pi,Fe \to \psi} B_{\psi \to \mu\mu} = (110 \pm 55)\text{nb} \qquad (X_L \geq 0.45)$$

$$\sigma_{p,Fe \to \psi} B_{\psi \to \mu\mu} = (41 \pm 21)\text{nb} \qquad (X_L \geq 0.375)$$

If we assume $\sigma_{X,Fe \to \psi} \propto A^{2/3}$, then we find for nucleon cross sections

$$\sigma_{\pi,N \to \psi} B_{\psi \to \mu\mu} = (7.5 \pm 3.8)\text{nb} \qquad (X_L \geq 0.45)$$

$$\sigma_{p^+,N \to \psi} B_{\psi \to \mu\mu} = (2.8 \pm 1.4)\text{nb} \qquad (X_L \geq 0.375)$$

If $\sigma_{X,Fe \to \psi} \propto A$ we obtain

$$\sigma_{\pi,N \to \psi} B_{\psi \to \mu\mu} = (2.0 \pm 1.0)\text{nb} \qquad (X_L \geq 0.45)$$

$$\sigma_{p^+,N \to \psi} B_{\psi \to \mu\mu} = (0.74 \pm .37)\text{nb} \qquad (X_L \geq 0.375)$$

Finally, if we assume that every π and proton interaction is with a single nucleon, and if we ignore the absorption of outgoing ψs, then the nucleon cross section is (e.g.) $\sigma_{\pi,N \to \psi} = P_{\pi,Fe}(\psi) \times \sigma_{\pi,N,inelas}$. Using $\sigma_{\pi,N,inelas} \approx 21$nb and $\sigma_{p,N,inelastic} \approx 32$ nb in this we find

$$\sigma_{\pi,N \to \psi} B_{\psi \to \mu\mu} = (3.3 \pm 1.7)\text{nb} \qquad (X_L \geq 0.45)$$

$$\sigma_{p^+,N \to \psi} B_{\psi \to \mu\mu} = (1.9 \pm .95)\text{nb} \qquad (X_L \geq 0.375)$$

We will tentatively use these final values. Using in addition measured values of the branching ratio for $\psi \to \mu^+ + \mu^-$ (6) we find

$$\sigma_{\pi,N \to \psi} = 48 \pm 24 \text{ nb/nucleon} \qquad (X_L \geq 0.45)$$

$$\sigma_{p,N \to \psi} = 27 \pm 14 \text{ nb/nucleon} \qquad (X_L \geq 0.375).$$

Finally, assuming the parameterization of Eq. 3 holds for protons from $-1 \leq X_{Feynman} \leq 1$, we find

$$\sigma_{p,N \to \psi} = (0.55 \pm 0.36)\text{nb} \qquad (\text{all } X)$$

Low Mass Preliminary Results

I would like to go on now to more recent, and still tentative, results of our analysis in the mass region below the ψ. Caveats will be noted where appropriate, and error quotes will generally be omitted, since proper fitting procedures have not yet been followed. The mass region to be discussed, $1.2 \leq M_{\mu\mu} \leq 2.5$ GeV, has more pitfalls than the ψ region. The large mass yield in the ρ region (See Figs. 3 and 4) opens the possibility that artifacts of the apparatus can result in a small fraction of the low mass peak being "scattered" into a higher mass tail. The possibilities of such artifacts must be carefully considered and this has not yet been done.

The mass region $1.2 \leq M_{\mu\mu} \leq 2.5$ GeV has been acceptance corrected. Figures 8 and 9 show the resulting mass spectra, for $X_L \geq 0.5$, on a log-log plot. The mass spectrum below 2.5 GeV is well fitted with a straight line, indicating a cross section of the form

$$\frac{d\sigma}{dM} \propto M^{-n} \qquad (7)$$

Both the proton and pion data are fit with a value of $n \sim 6$. Our preliminary analysis indicates that the result of resolution effects on this value should not be significant.

Fig. 8 Fig. 9

We may also fit this intermediate mass region to the form of Eq. 3. The results of such fits are given in Table 2.

Table 2

Intermediate Mass Region $(1.2 \leq M_{\mu\mu} < 2.5 \text{ GeV})$

(Note: All data in this table are preliminary. Proper fitting has not been done, and a search for instrumental artifacts has not been completed).

Cross section form	π^-	p^+
M^{-n}	$n_\pi \sim 6$	$n_p \sim 6$
e^{-aX_L}	$a_\pi \sim 3.7$	$a_p \sim 7.9$
$e^{-bp_\perp^2}$	$b_\pi \sim 1.2 \text{ GeV}^{-2}$	$b_p \sim 1.2 \text{ GeV}^{-2}$

Finally, we may compare the probabilities of production of a dimuon in the intermediate mass region, for $X_L \geq 0.5$, by protons and by pions. In this case,

$$R \equiv \frac{P_\pi(1.2 \leq M_{\mu\mu} \leq 2.5 \text{ GeV})}{P_p(1.2 \leq M_{\mu\mu} \leq 2.5 \text{ GeV})} \sim 5 \pm 1 \qquad (X \geq 0.5)$$

This result is consistent with the π/p production ratio found in the ψ region.

In the mass region below 1.2 GeV our analysis is incomplete. We have not yet corrected the data for acceptance. I would make two comments upon this region.

First, the shape of the $p_\perp^2$ spectrum produced by π's is essentially the same as that produced by protons. We see in Tables 1 and 2 that this is, within quoted errors, also true of the higher mass regions. i.e., it appears that the $p_\perp$ spectra of dimuons, unlike their X_L spectra, are invariant to the projectile used.

Secondly, at the present stage of our analysis, it does not appear that the ρ alone can account for the low mass peak, since the width of the peak in the data is broader than we would expect. This conclusion is tentative. Our confidence in our Monte Carlo simulation has been developed mainly in the ψ region, and we must repeat the process in the lower mass region.

Footnotes

* The work described herein was supported in part by the National Science Foundation under Grant MPS70-02059A5.

† Sloan Foundation Fellow.

□ The work described herein comprises part of a dissertation submitted in partial fulfillment of the requirements of the degree of Doctor of Philosophy.

1) J. J. Aubert et al., Phys. Rev. Lett. 33, 1404 (1975) and
J. E. Augustin, et al., Phys. Rev. Lett. 33, 1406 (1975).

2) G. Blanar, et al., Phys. Rev. Lett. 35, 346 (1975).

3) B. Knapp, et al., Phys. Rev. Lett. 34, 1040 (1975).

4) B. Knapp, et al., Phys. Rev. Lett. 34, 1044 (1975).

5) A portion of the factor of 3.6 by which our measured probabilities exceed those of Ref. 4 may be due to physics. If the ψ production cross section is, for example, proportional to A instead of $A^{2/3}$, one would expect the probability per incident beam particle to be about twice as large in Fe as in Be. This would make the discrepancy in the measured cross sections a factor of 1.8 rather than 3.6.

6) A. M. Boyarski, et al., Phys. Rev. Lett. 34, 1357 (1975).
J. A. Kadyk, et al., LBL Report #3687 (unpublished).

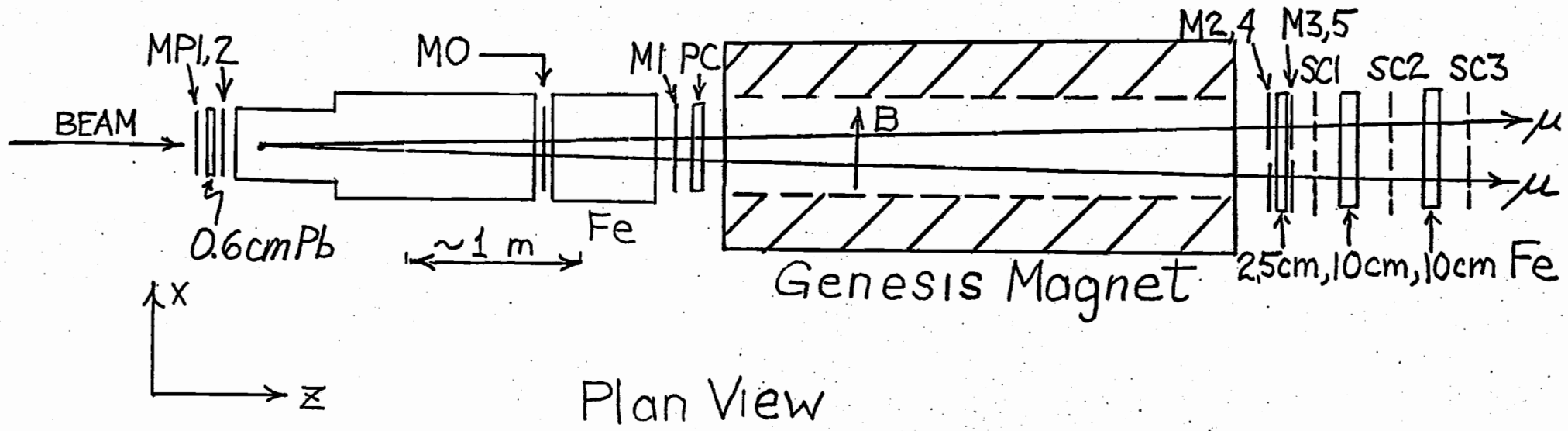

Plan View

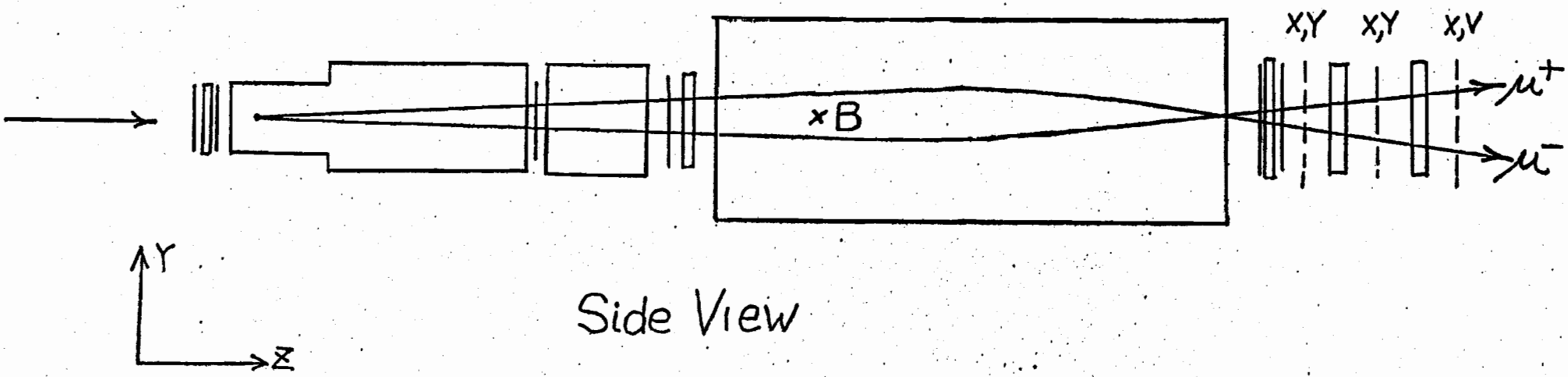

Side View

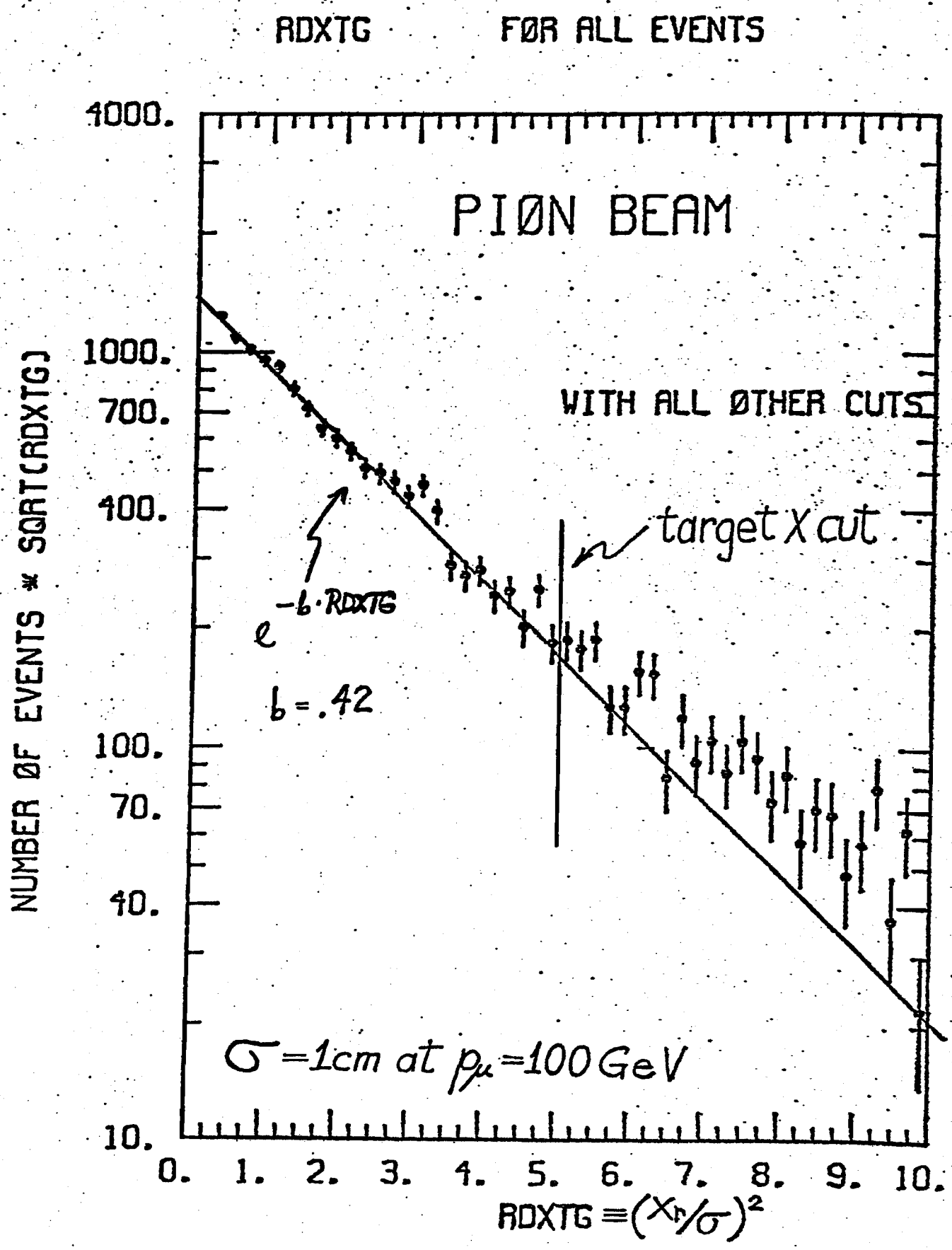
RDXTG FØR ALL EVENTS
PIØN BEAM
WITH ALL ØTHER CUTS
target X cut
$e^{-b \cdot RDXTG}$
b = .42
σ = 1cm at p_μ = 100 GeV
NUMBER ØF EVENTS * SQRT(RDXTG)
RDXTG ≡ $(X_t/\sigma)^2$
4000.
1000.
700.
400.
100.
70.
40.
10.
0. 1. 2. 3. 4. 5. 6. 7. 8. 9. 10.

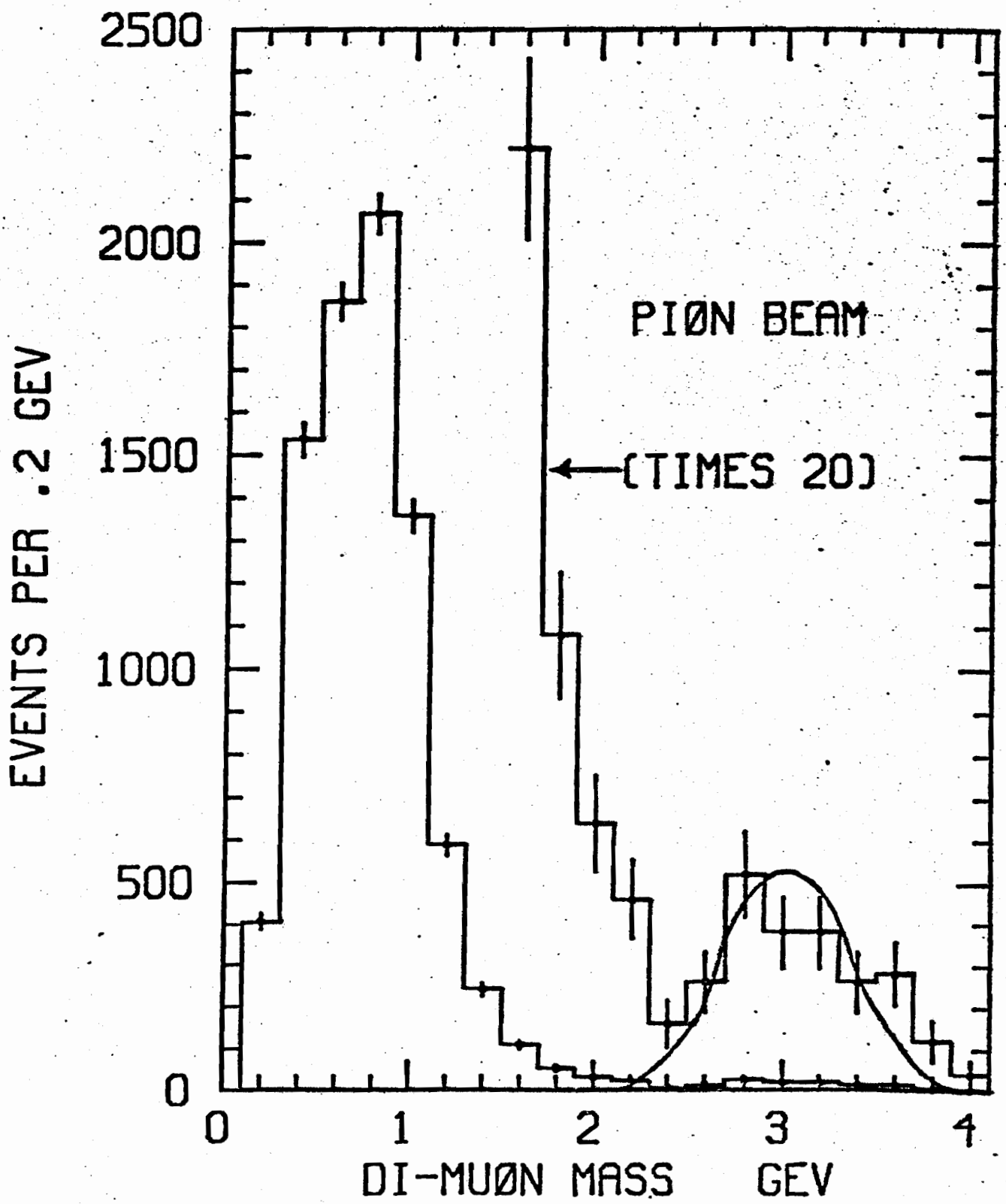
2500
2000
1500
1000
500
0
EVENTS PER .2 GEV
PIØN BEAM
(TIMES 20)
0
1
2
3
4
DI-MUØN MASS GEV

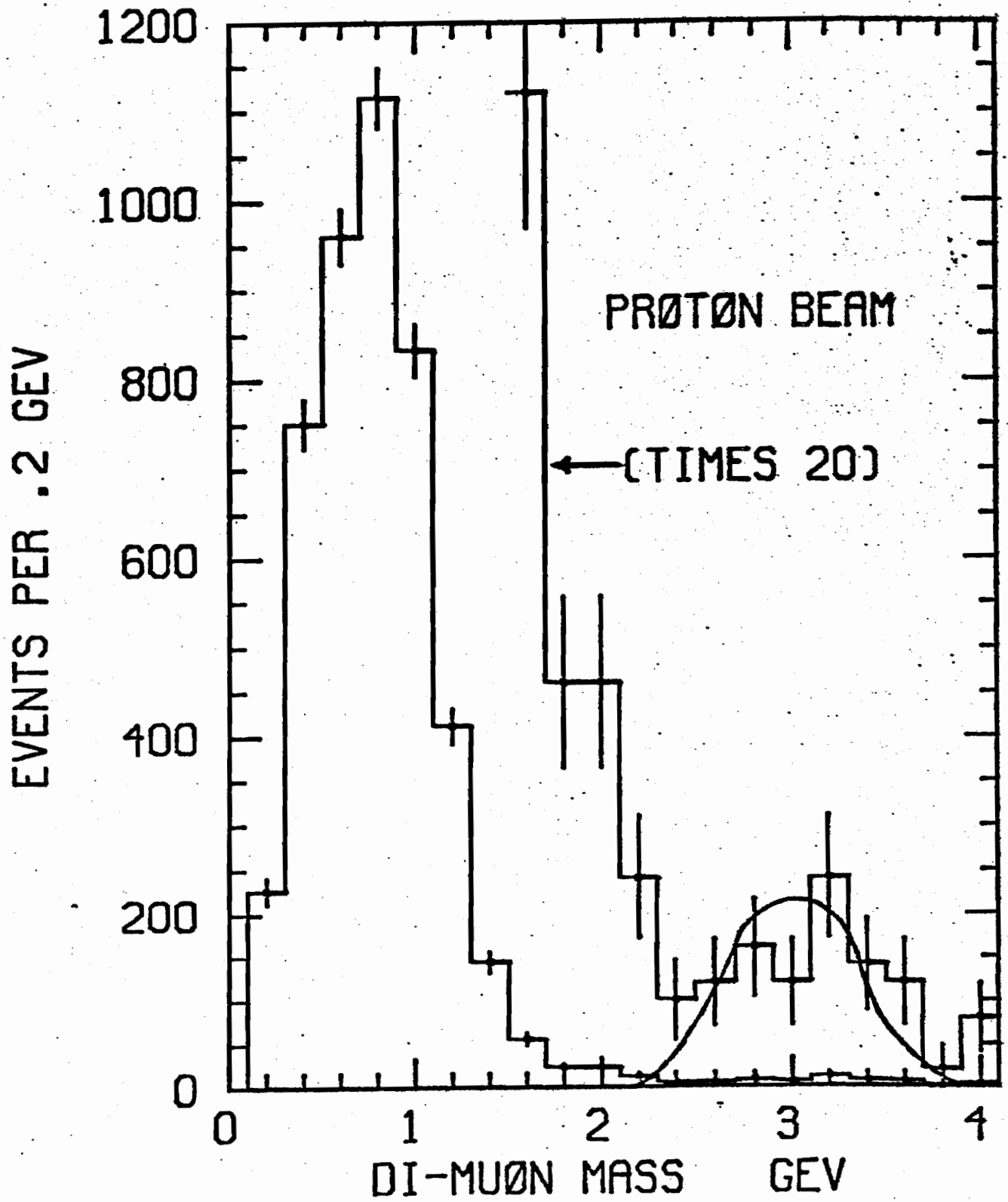
1200
1000
800
600
400
200
0
EVENTS PER .2 GEV
PRØTØN BEAM
(TIMES 20)
0
1
2
3
4
DI-MUØN MASS GEV

DI-MUØN LØNGITUDINAL MØMENTUM WEIGHTED

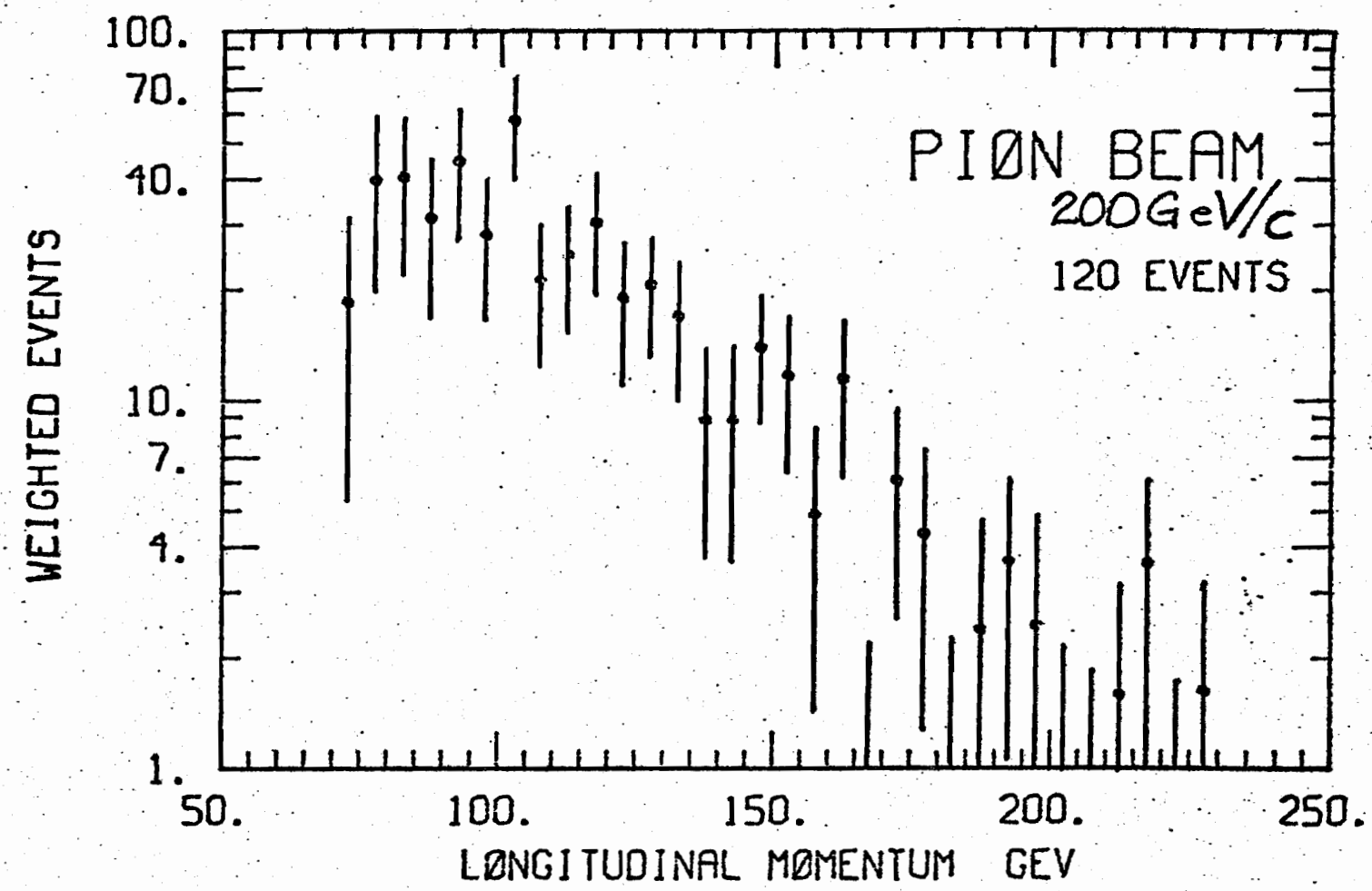

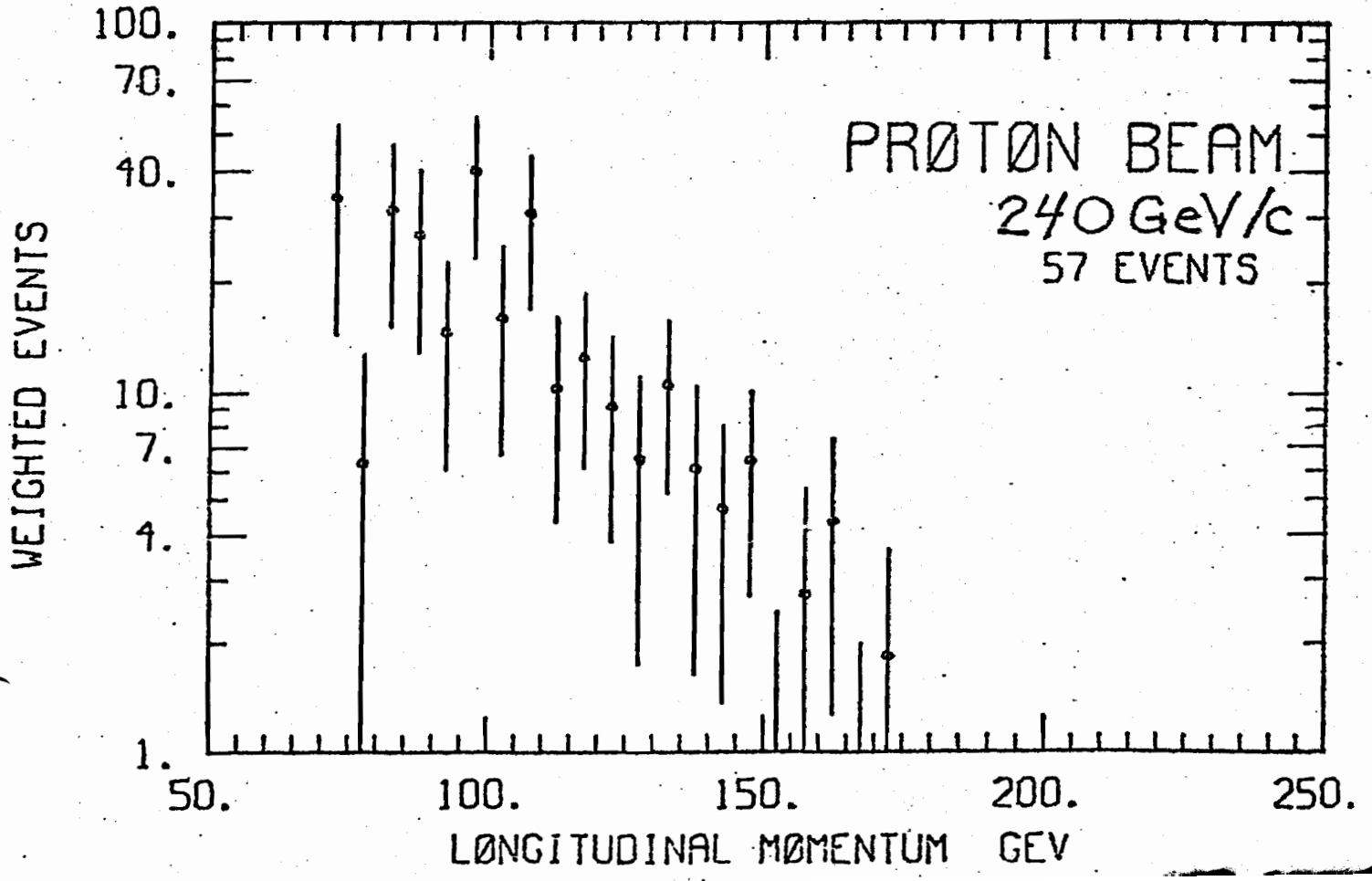

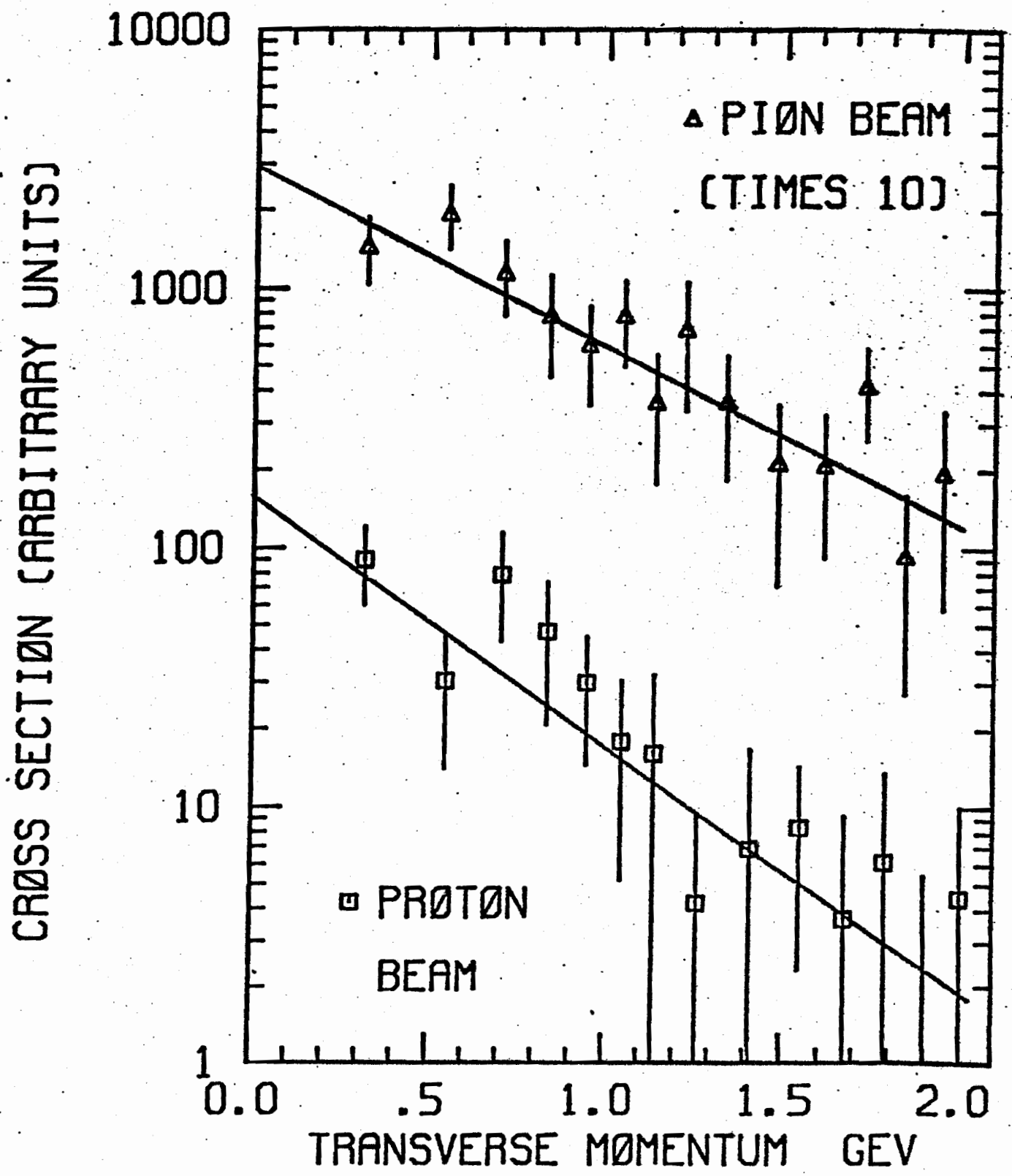
10000
1000
100
10
1
CRØSS SECTIØN (ARBITRARY UNITS)
PIØN BEAM
(TIMES 10)
PRØTØN
BEAM
0.0
.5
1.0
1.5
2.0
TRANSVERSE MØMENTUM GEV

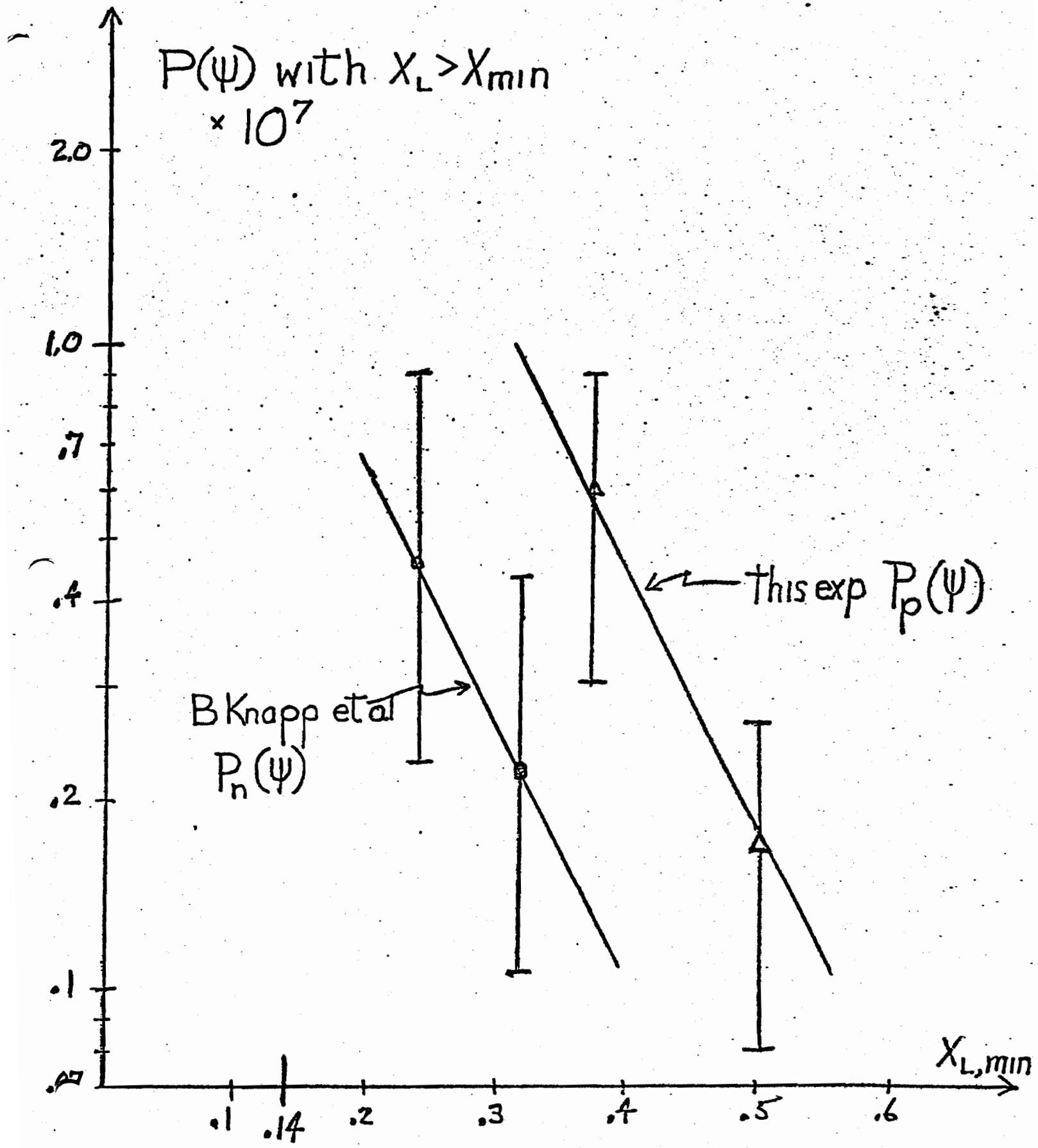
P(ψ) with $X_L > X_{min}$
× 10^7
2.0
1.0
.7
.4
.2
.1
.05
.1
.14
.2
.3
.4
.5
.6
$X_{L,min}$
This exp $P_p(\psi)$
B Knapp et al
$P_n(\psi)$

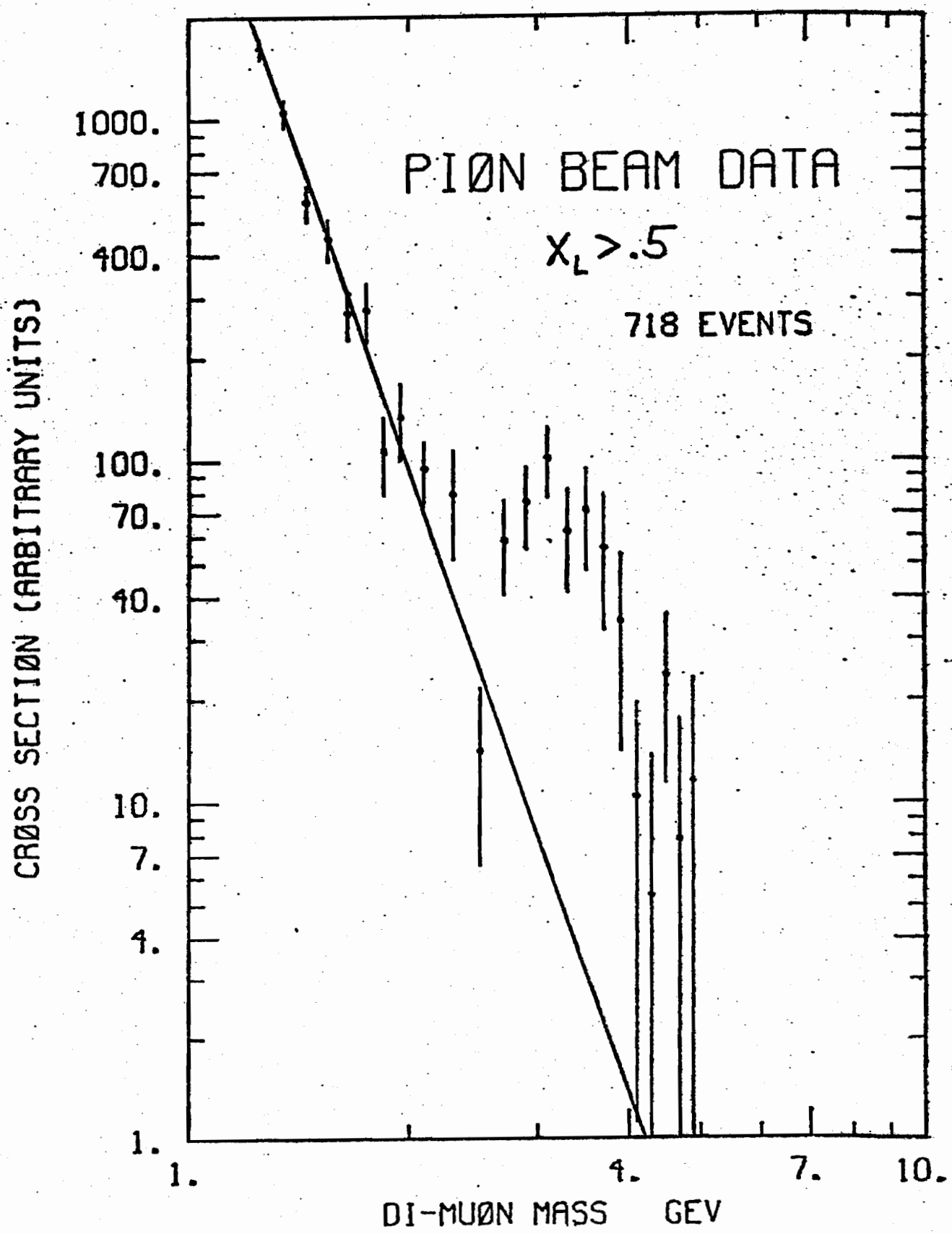
PIØN BEAM DATA
$X_L > .5$
718 EVENTS
CRØSS SECTIØN (ARBITRARY UNITS)
1000.
700.
400.
100.
70.
40.
10.
7.
4.
1.
1.
4.
7.
10.
DI-MUØN MASS GEV

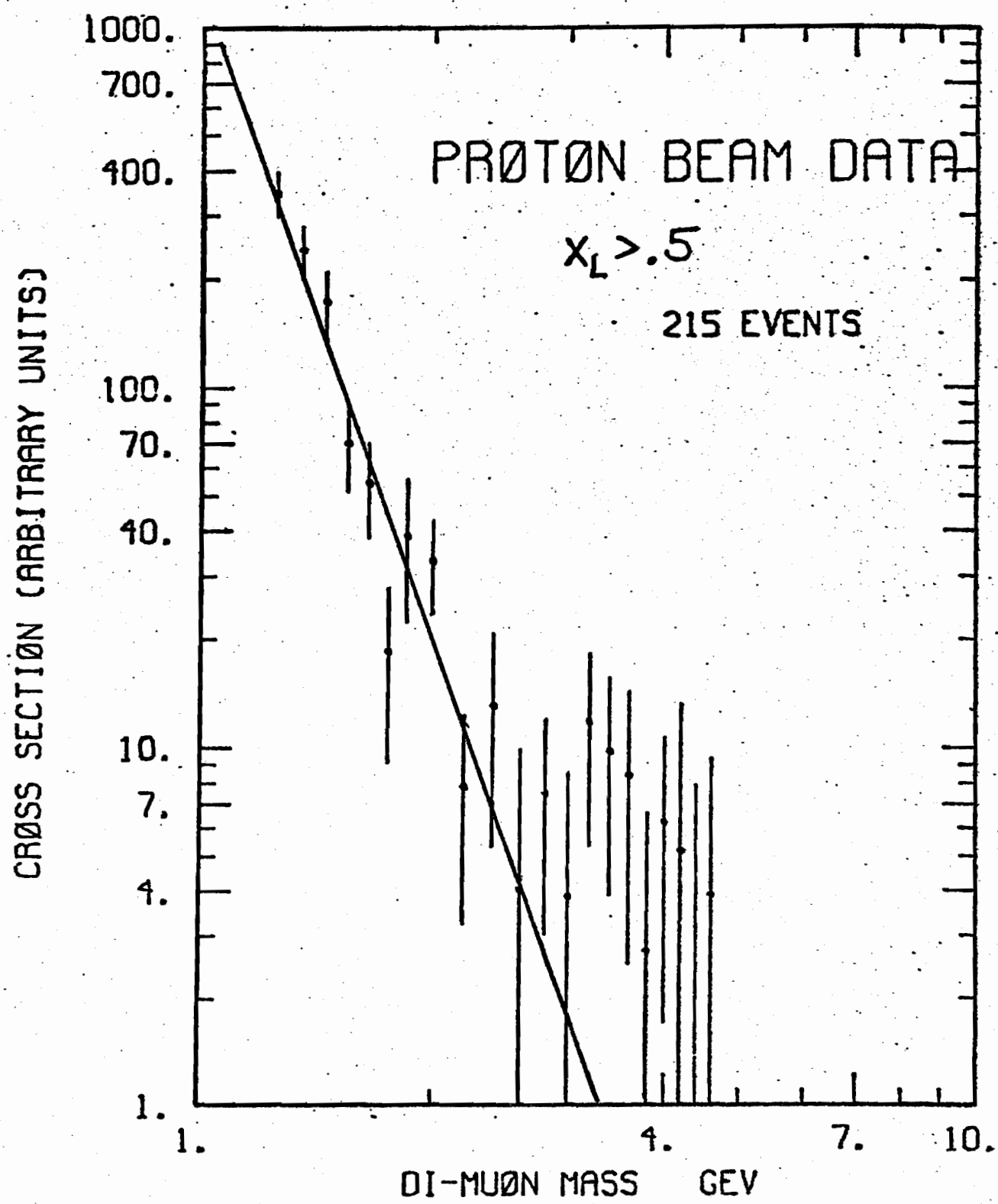
PRØTØN BEAM DATA
$x_L > .5$
215 EVENTS
CRØSS SECTIØN (ARBITRARY UNITS)
1000.
700.
400.
100.
70.
40.
10.
7.
4.
1.
1.
4.
7.
10.
DI-MUØN MASS GEV